Zhou, S.; Xu, X.; Ma, N.; Jung, F.; Lendlein, A.:

Influence of sterilization conditions on sulfate-functionalized polyGGE.

In: Clinical Hemorheology and Microcirculation. Vol. 79 (2021) 4, 597 - 608.

First published online by IOS: 19.08.2021

https://dx.doi.org/10.3233/CH-211241

Influence of sterilization conditions on sulfate-functionalized polyGGE

Shuo Zhou[1, 2], Xun Xu[1, 3], Nan Ma[1, 3, 4], Friedrich Jung[1, 3], Andreas Lendlein[1, 2, 3, 4, *]

[1]Institute of Active Polymers, Helmholtz-Zentrum Hereon, 14513 Teltow, Germany

[2]Institute of Chemistry, University of Potsdam, 14476 Potsdam, Germany

[3]Berlin-Brandenburg Centre for Regenerative Therapies, Helmholtz-Zentrum Hereon, 14513 Teltow, Germany

[4]Institute of Chemistry and Biochemistry, Freie Universität Berlin, 14195 Berlin, Germany

* To whom correspondence should be addressed:

Prof. Dr. Andreas Lendlein, Institute of Active Polymers, Helmholtz-Zentrum Hereon, Kantstr. 55, 14513 Teltow, Germany email: andreas.lendlein@hereon.de

Abstract

Sulfated biomolecules are known to influence numerous biological processes in all living organisms. Particularly, they contribute to prevent and inhibit the hypercoagulation condition. The failure of polymeric implants and blood contacting devices is often related to hypercoagulation and microbial contamination. Here, bioactive sulfated biomacromolecules are mimicked by sulfation of poly(glycerol glycidyl ether) (polyGGE) films. Autoclaving, gamma-ray irradiation and ethylene oxide (EtO) gas sterilization techniques were applied to functionalized materials. The sulfate group density and hydrophilicity of sulfated polymers were decreased while chain mobility and thermal degradation were enhanced post autoclaving when compared to those after EtO sterilization. These results suggest that a quality control after sterilization is mandatory to ensure the amount and functionality of functionalized groups are retained.

Introduction

Cardiovascular disease remains the leading cause of global mortality. Hypercoagulation disorders such as venous thromboembolism is the second most frequent cardiovascular disorder followed by myocardial infarction. Hypercoagulation disorders are inherited, and can be acquired by various external factors such as surgery, pregnancy, inflammation, malignancy and infection [1-3].

Sulfate, a key component of extracellular matrix and one of the most abundant anions in the blood, are involved in the biosynthesis of various essential body compounds. It presents in a variety of forms, drives numerous biological functions and metabolic events [4,5]. More and more studies have revealed that the deficiency of sulfate contributes to the pathogenesis of cardiovascular diseases including chronic heart failure, atherosclerosis, hypercoagulation [6-8].

A special form of sulfate produced by red blood cells or platelets is cholesterol sulfate, which accumulates around the cells and creates a negatively charged shield to enable their smooth passage through capillaries, to prevent the blood cells from rupturing and to regulate platelet adhesion [9,10]. The major form of sulfate in the extracellular matrix is sulfated glycosaminoglycan (GAG) including chondroitin sulfate, heparan sulfate, and keratan sulfate [11]. Their biological activities with distinct regulatory functions in tissue mechanical property, cell adhesion, growth, proliferation, differentiation, anticoagulation, wound healing, tumorigenesis and antiviral effects rely on the sulfation degree of GAGs [12-15]. Heparin, as a more sulfated variant of heparan sulfate, exhibits a prominent and effective anticoagulant and antithrombotic feature due to sulfate mediated conformation change of antithrombin III [16-18]. In addition, it was demonstrated that the heparin can inhibit the SARS-COV-2 viral entry and may play a critical role in treating SARS-COV-2 triggered hypercoagulation [15,19].

Polymer-based implants, such as polymeric stents, interventional devices and polymeric vaccine adjuvants are widely used. Hypercoagulation with thrombus formation at the interfaces between implant materials and their physiological environment are a major issue leading to the failure of the medical applications of polymer-based biomaterials [20,21]. For blood contact materials, surface properties attract more attention than bulk properties. Physicochemical surface properties including wettability, surface charge, topography, stiffness as well as functional groups exposed at the interface are considered to strongly influence protein adsorption, and regulate the blood cell adhesion and activation [22-25]. Importantly, surface

contamination of microorganism generally triggers hypercoagulation as a consequence of direct activation of coagulation factors or immune reactivities [26].

Here, a sulfate-functionalized surface based on the poly(glycerol glycidyl ether) (polyGGE) was designed and created in order to improve hemocompatibility, which shall mimic the biofunctionality of the heparin. Surface composition, hydrophilicity and thermal properties of sulfate-functionalized polyGGE were evaluated. Three commonly used sterilization techniques, autoclaving, gamma-ray irradiation and ethylene oxide (EtO) gas sterilization, were compared to verify the appropriate sterilization condition, which was capable of preserving the functional sulfates on polyGGE surface.

Materials and Methods

Sulfation of polyGGE surface

Polymerization of glycerol glycidyl ether (GGE, Raschig GmbH, Ludwigshafen am Rhein, Germany) was carried out using a one-step cationic ring opening polymerization in the presence of 30 min UV exposure and quenching with 1 mol/L KOH aqueous solution for 24 h [27]. PolyGGE films were reacted with 5 wt% sulfamic acid in N-Methyl-2-pyrrolidone (all sulfating agents were purchased from Sigma-Aldrich GmbH, Steinheim, Germany), which was pre-heated to 90 °C while stirring. After reaction for 5, 15, 30, 45, 60 min, bulk films were rinsed with distilled water and immersed in saturated NaCl solution at room temperature overnight. The residual solvent was extracted by washing with ethanol (Sigma-Aldrich GmbH, Steinheim, Germany) at room temperature for 3 days. The sulfate functionalized polyGGE was dried at room temperature in a high vacuum for one week until the weight reached a constant value.

Synthesis of poly (hydroxyethyl acrylate) (PHEA) model system

Hydroxyethyl acrylate monomers were bulk polymerized between glass plates with 0.5 wt% azo-bis-isobutyronitrile as an initiator and 0.1 wt% of ethylene glycol dimethacrylate as a cross-linking agent (all agents were purchased from Sigma-Aldrich GmbH, Steinheim, Germany). Polymerization was carried out at 60 °C for 24 h. Poly(hydroxyethyl acrylate) (PHEA) hydrogels were extracted with ethanol in Soxhlet for one week before sulfation and dried at 60 °C in a high vacuum for one week until the weight reached a constant value. An

identical sulfation protocol for polyGGE was applied to PHEA, except for the reaction time which was prolonged to 24 h. The sulfate functionalized materials were named PHEAS.

Sterilization

Autoclaving was set under following conditions: 120 °C, 20 min, 2 bar using a FVA A1 autoclave (Integra Biosciences, Biebertal, Germany). Gamma-ray irradiation was performed with Gammacell 1000 Elite (Best Theratronics, Ottawa, Canada). Samples were exposed to Cs137 gamma-ray at a dose of 25 kGy for 24 h. Ethylene oxide (EtO) sterilization were performed in an automated EtO sterilizer (SteriVit 100, DMB Apparatebau, Wörrstadt, Germany) with a gas (6 vol% EtO in 94 vol% CO_2) exposure at 45 °C and 75 vol% relative humidity for 180 min, followed by desorption in more than 250 pressure/vacuum cycles between + 0.6 bar and − 0.76 bar over 12 h.

Attenuated total reflection Fourier transform infrared (ATR-FT-IR) spectroscopy

Functionalized surface was analyzed by ATR-FT-IR spectroscopy (Nicolet IR 6700, Thermo Fisher Scientific, Waltham, USA). 50 scans were performed for each measurement. The polymers were analyzed in the absorbance range from 400 to 4000 cm^{-1} with a resolution of 2 cm^{-1}.

Thermogravimetric analysis (TGA)

The thermal degradation of polymer and sulfate functionalized polymers before and after sterilization was conducted on a TG209 instrument (Netzsch, Selb, Germany) with a constant heating rate of 10 °C/min between 25 and 600 °C in a nitrogen atmosphere.

Differential scanning calorimetry (DSC)

DSC experiments were performed on DSC 204 Phoenix calorimeter (Netzsch, Selb, Germany). A heating-cooling-reheating cycle was performed using the same heating rate of 10 °C/min for all 3 cycles. Samples sealed in aluminum pans were heated up from -70 °C to 200 °C before the cooling run to -70 °C, followed by the second heating run up to 200 °C. The glass transition temperature (T_g) was determined from the second heating run.

X-ray photoelectron spectroscopy (XPS)

The measurement was conducted with a Kratos Axis Ultra instrument (Kratos Analytica, Manchester, UK) using a monochromatic Al Kα beam source (1486.6 eV), whereby the signal was averaged over an area of 0.3 mm × 0.7 mm. Survey scans were recorded with a pass energy

of 160.0 eV, while regional spectra of carbon (C 1s), oxygen (O 1s) were taken with 20.0 eV at 300 W. A semi-quantitative evaluation was carried out based on the fractional peak areas and using the Casa XPS software (Version 2.3.16, Casa Software Ltd., Teignmouth, UK). All values were given as atom% (at%).

Toluidine blue O (TBO) staining

The amount of sulfate groups on functionalized polyGGE (prepared as round films with thickness 45 mm and diameter 13 mm) was determined by a TBO (Sigma-Aldrich GmbH, Steinheim, Germany) staining. Polymer films were incubated in 1 mL of a freshly prepared solution of 0.04 wt% TBO in aqueous 0.01 M HCl/ 0.2 wt% NaCl. Then, the samples were gently shaken at 37 °C for 4 h and rinsed twice with demineralized water. During this process, the sulfate/TBO complex was formed on the sample surface. Following this, 10 mL of a 4/1 (v/v) mixture of ethanol and aqueous 0.1 mol/L NaOH was added, and the sulfate/TBO complex dissolved and released into the fluid phase. After complete dissolution of the complex, 200 µL of supernatant was added to a 96-well microplate, and the optical density (OD) value was obtained with a microplate reader Infinite 200Pro (Tecan, Wiesbaden, Germany) at 630 nm wavelength. The OD value was used to calculate the amount of sulfate from a calibration curve with known TBO concentration.

Water contact angle measurement

DSA 100 (Krüss GmbH, Hamburg, Germany) was applied for determine the water contact angles of polyGGE, sulfate functionalized polyGGE with and without sterilization using the captive bubble method. All samples were equilibrated for 24 h in deionized water at room temperature. Advancing and receding contact angles were measured by stepwise withdrawing/adding of air from/to the captured bubble, while the bubble was increased with each measurement cycle from 2 to 5 mm in diameter. Ten measurements on two different locations were performed on three samples.

Water uptake ability

PHEA and sulfate functionalized PHEA before and after sterilizations swelled in distilled water for 24 h to reach a water uptake equilibrium. Weight at equilibrium was recorded as W_{eq}. Samples were dried at 60 °C in vacuum until no further weight decrease was found. Weight at dry state was recorded as W_d. Water uptake ability was calculated as $\frac{W_{eq}-W_d}{W_d} \times 100\ \%$.

Statistics

All data were presented as mean value ± standard deviation. GraphPad Prism v6.02 software (GraphPad Software Inc., San Diego, USA) was used for statistical analysis. One-way analysis of variance (ANOVA) with Bonferroni's multiple comparison tests were applied for the comparisons of the individual groups. At least three independent biological replicates were involved. p value < 0.05 were considered statistically significant.

Results and Discussion

Saturated NaCl stabilized sulfate-functionalized polyGGE films

Sulfamic acid, a mild reagent for producing ammonium sulfates from alcohols or ethoxylated alcohols, was selected for sulfate grafting of polyGGE surface due to its specifical prevention of the formation of mixed sulfate-sulfonate compounds [28,29]. Here, polyGGE films were pretreated with ethanol in soxhlet extractor for two weeks. As illustrated in **Fig. 1A**, sulfating of the films was carried out by a reaction between polyGGE and 5 wt% sulfamic acid in N-Methyl-2-pyrrolidone solution at 90 °C for at least 5 min. Upon heating, sulfamic acid reacts with alcohol groups to form the corresponding organosulfates ($R\text{-}O\text{-}SO_3^-$). However, loss of organosulfates was found during the storage of the ammonium polyGGE sulfates in aqueous condition. This is probably because H^+ formation at the solid-aqueous interface from the hydrolysis of the NH_4^+ aids the cleavage of the sulfate [30].

In order to stabilize the sulfate groups, the sulfate-functionalized polyGGE (polyGGE_S) films with the increased sulfating reaction times (5, 10, 15, 30, 45 and 60 min) were further treated with saturated NaCl for 24 h, in which process, NH_4^+ ions were replaced by Na^+ (**Fig. 1A**). To evaluate the chemical composition changes of the stabilized polyGGE_S5, _S10, _S15, _S30, _S45 and _S60, ATR-FT-IR spectroscopy has been performed. Post one week storage of samples, apparently new vibration signals were found at the wavenumbers 610 and 1225 cm^{-1} (asymetric stretching of S=O), 945 and 1008 cm^{-1} (sysmetric stretching of S=O), and 780 cm^{-1} (-C-O-S-) (**Fig. 1B**). These peaks corresponded well with the expected signals in comparison to the signals of the pure polyGGE and the functionalization agents. Moreover, the signal intensity of these peaks enhanced with an increasing reaction time of polyGGE and sulfamic acid, especially the occurrence and the increasing of the peak signal at 780 cm^{-1} (-C-O-S-), which confirmed the successful covalent binding of hydroxyl groups and sulfates and increased density of grafted sulfate groups on polyGGE and suggesting a successfully stabilization of materials.

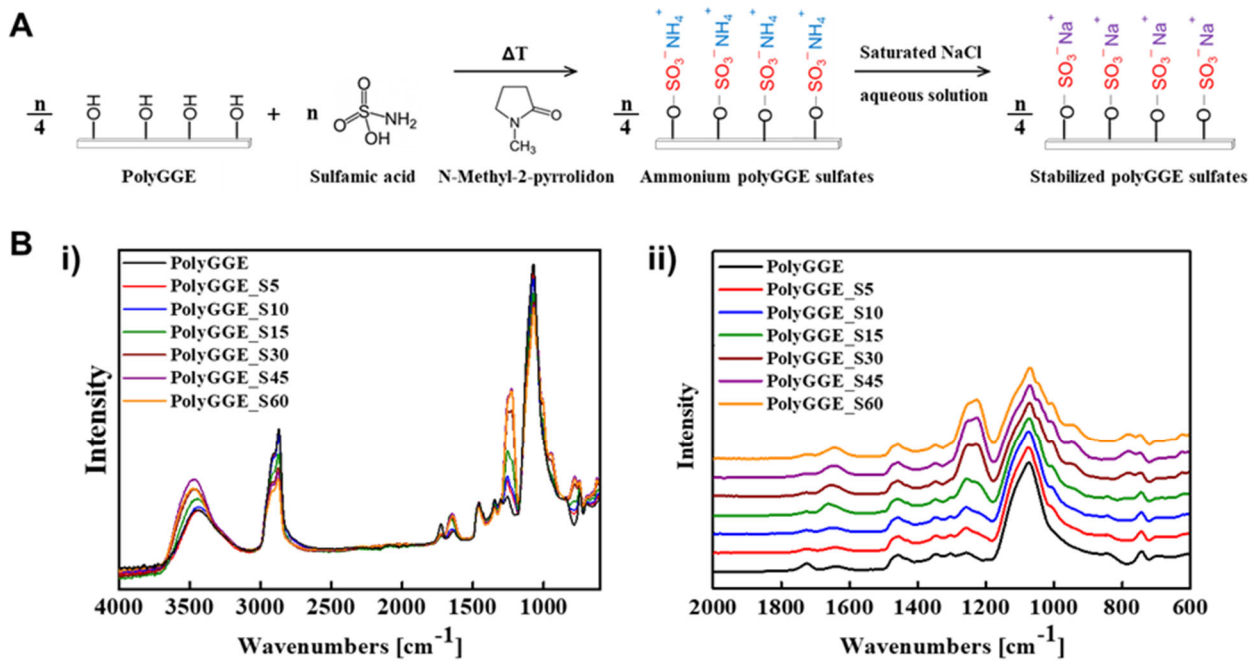

Fig. 1. Stabilization of sulfate-functionalized polyGGE. A. Reaction scheme of functionalization and stabilization processes of polyGGE. **B.** ATR-FT-IR spectra of polyGGE and polyGGE_S5, polyGGE_S10, polyGGE_S15, polyGGE_S30, polyGGE_S45 and polyGGE_S60 after saturated NaCl treatment. **i**), spectrum in the range of 500-4000 cm^{-1}; **ii**), zoom-in spectrum in the range of 600-2000 cm^{-1}.

Sulfate-functionalized polyGGE films were thermally stable at body temperature

Sulfate-functionalized polyGGE with longer reaction times (more than 15 min) yielded more yellowish bulk polymers. Color change is thought to be an indicator of potential sulfonation with sulfuric acid, which is closely related to sulfamic acid [31,32]. PolyGGE films after 30, 45 and 60 min sulfation (polyGGE_S30, _S45 and _S60) showed apparently different levels of cracking. In contrast to that, polyGGE films post 5, 10 and 15 min sulfation (polyGGE_S5, _S10 and _S15) had no visible cracks (**Fig. 2A**). On one hand, this might attribute to the uptake of N-Methyl-2-pyrrolidone, which elicits the changes in the internal stress during swelling and deswelling process. On the other hand, it can be caused by the undesired modification that takes place inside the polymer network. Therefore, to ensure the modification only occurred on the surface of the bulk and to avoid the influence of the potentially changed bulk properties, polyGGE_S5, _S10 and _S15 were used for the further investigation.

To evaluate the effect of sulfation on the thermal stability of polyGGE_S5, _S10 and _S15, TGA curves of non-functionalized and sulfate-functionalized polyGGE were obtained under nitrogen atmosphere. Starting from 100 °C to 300 °C, a first step of weight loss of 9.7% was

found for polyGGE_S15 while polyGGE, polyGGE_S5 and _S10 exhibited weight losses of 5.5%, 8.3% and 7.7% (**Fig. 2B**). The first part of the weight loss is associated with small molecules already existing during the synthesis and the dechlorination process. However, the weight losses of sulfate-functionalized polyGGE films were relatively higher than non-functionalized polyGGE, indicating a potential decomposition process might take place during such heating period, which might be the loss of sulfates. With an increasing of the temperature, a drastic degradation process occurred at 300 °C for the bulk materials and lasted until 600 °C. 92.4%, 92.4%, 90.62% and 91.8% of weight loss were determined for polyGGE, polyGGE_S5, _S10 and _S15, respectively (**Fig. 2B**). Although TGA is not capable of confirming the loss of sulfates, it provides a hint that sulfate groups are not thermally stable over 100 °C.

To further study whether the sulfation affect the thermal properties of polyGGE, DSC measurement was performed. Independent of the sulfation time, T_g of polyGGE_S5 (32 °C), _S10 (35 °C) and _S15 (33 °C) were comparable with that of the non-functionalized polyGGE (33 °C) (**Fig. 2C**), suggesting the sulfation process did not influence the mobility of the original polymer chain in bulk material. The sulfate-functionalized polyGGE films were able to retain their pliable rubbery state at body temperature.

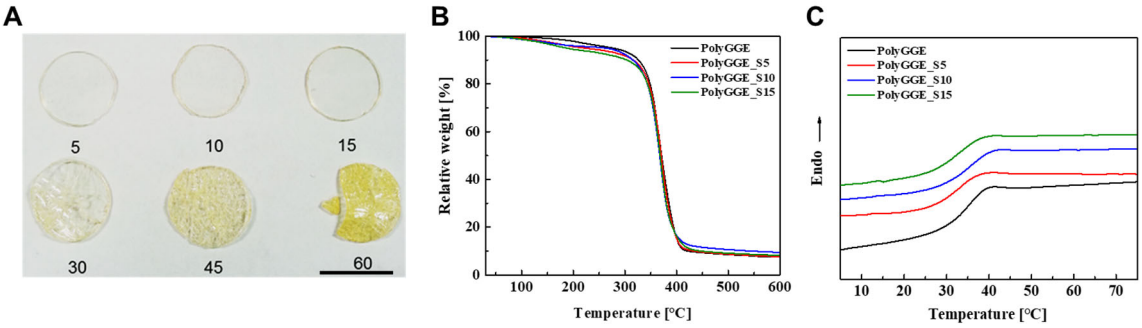

Fig. 2. Thermal properties of sulfate-functionalized polyGGE. A. Representative image of polyGGE_S5, S10, S15, S30, S45 and S60 after saturated NaCl treatment. Scale bar = 13 cm. TGA profiles (**B**) and DSC heating curves (**C**) of polyGGE, polyGGE_S5, S10 and S15.

Sulfation took place on the surface of polyGGE

Both the surface and the cross-section of polyGGE_S15 were analyzed by XPS to verify, at which location sulfation took place. The specific peaks of S (**Fig. 3A**) and Na (**Fig. 3B**) exhibited on XPS spectra and the semi-quantitative data (**Table 1**) confirmed that neither S nor Na appeared in the cross-section of the PolyGGE_S15 while 1.67 at% of S and 0.8 at% of Na were detected on the surfaces. Moreover, the atom percentage of oxygen was increased from

23.37 at% to 28.06 at% with a difference of 4.59 at%, which was almost 3-fold as the atom percentage of S (1.67 at%) in line with the chemical structure of -SO_3. Although the polymer was intensively washed by ethanol, fluorine from the photoinitiator during polyGGE synthesis was traced from the surface (0.28 at%) and the cross-section (0.40 at%) (**Table 1**). These results suggested that sulfation only existed on the surface but not inside the bulk of the polyGGE_S15.

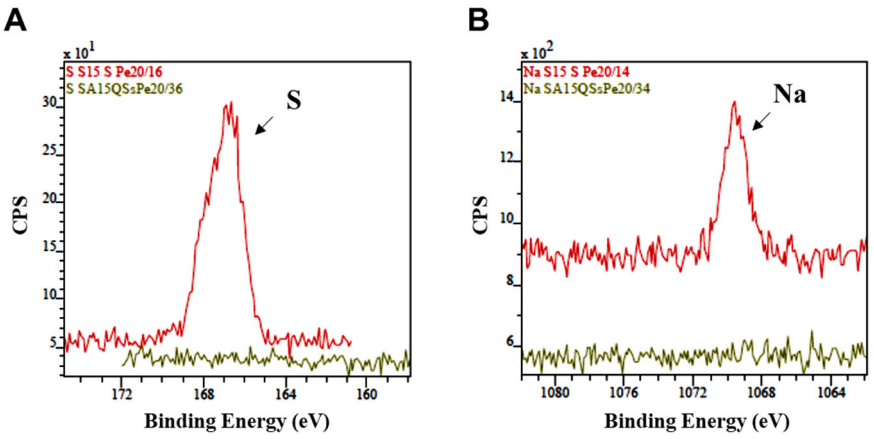

Fig. 3. Sulfate functionalization occurred on the surface of polyGGE. XPS spectra of region scan of S (**A**) and Na (**B**) on the surface (red) and cross section (yellow).

Table 1. Composition of polyGGE_S15 at surface and cross section

	C 1s	O 1s	Cl	S	Na	F
PolyGGE_S15	[at%]	[at%]	[at%]	[at%]	[at%]	[at%]
Surface	63.39	28.06	2.73	1.67	0.80	0.28
Cross section	72.49	23.37	1.05	-	-	0.40

Ethylene oxide (EtO) sterilization preserved the sulfation of polyGGE

An appropriate sterilization method needs to be defined for the downstream biological evaluation of sulfate-functionalized polyGGE films. This basically requires the stability preservation of the functionalized sulfate. To this end, three clinical-relevant sterilization methods including autoclaving, EtO gas and gamma-ray irradiation were applied to sterilize the polyGGE without sulfation, and their physical and thermal characteristics were investigated.

As shown in the ATR-FT-IR spectra, peaks for S=O located at 1225 cm^{-1} and 1008 cm^{-1}, and the -C-O-S- bonds at 780 cm^{-1} were observed for both polyGGE_S15_G and polyGGE_S15_E and the intensity of these peaks were identical to the unsterilized polyGGE_S15. Nevertheless, the signals of S=O and -C-O-S- bonds were diminished for polyGGE_S15_A, indicating the loss of covalently bonded sulfates caused by the autoclaving (**Fig. 4A**). Similar phenomenon has been reported for heparin. A decrease in the amount of sulfate groups in heparin's abundant tri-sulfated disaccharide repeating unit was found post autoclaving. The loss of the sulfates reduces the binding affinity of heparin to ATIII and thrombin, and impairs their anti-coagulate activity [33].

Density of grafted sulfate groups can be quantified by an indirect staining with toluidine blue O (TBO) [34]. TBO as a positively charged dye can interact with the negatively charged functional groups via electrostatic interaction, which can be dissociated by the addition of acid. The sulfate densities after autoclaving (polyGGE_S15_A) decreased remarkably from 69 ± 7 nmol/cm^2 to 11 ± 3 nmol/cm^2 compared to untreated polyGGE_S15. EtO treated and gamma-ray irradiated sulfate-functionalized polyGGE showed no significant changes with untreated group (70 ± 5 nmol/cm^2 for polyGGE_S15_E and 63 ± 8 nmol/cm^2 for polyGGE_S15_G) (**Fig. 4B**).

The influence of sterilization on the surface hydrophilicity was further studied by water contact angle measurements. PolyGGE_S15 (Θ_{adv} = 36±8°) exhibited more surface property than polyGGE (Θ_{adv} = 71±3°). Decreased hydrophilicity (Θ_{adv} = 67±1°) was determined for polyGGE_S15_A in contrast to the polyGGE_S15_E (Θ_{adv} = 35±8°) or polyGGE_S15_G (Θ_{adv} = 37±9°), which was comparable with the unsterilized polyGGE_S15 (**Fig. 4C**). The decreased hydrophilicity on polyGGE_S15_A gives a strong evidence for the loss of the sulfates after autoclaving.

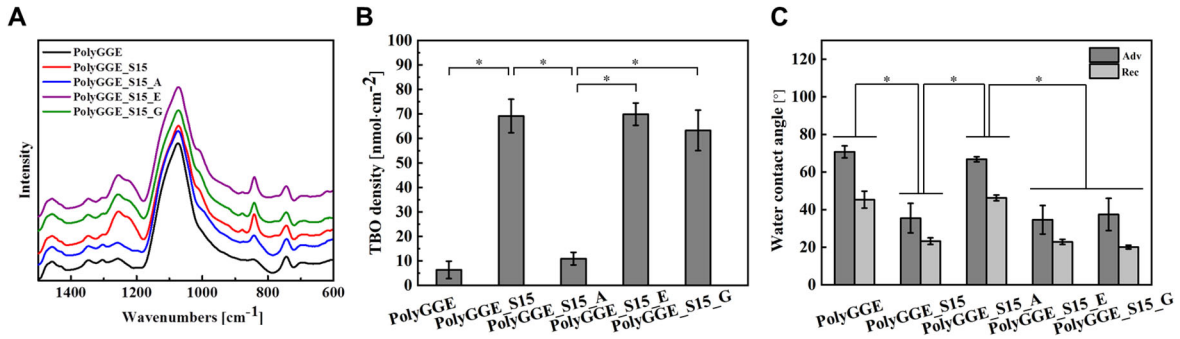

Fig. 4. Autoclaving decreased the amount and density of sulfates in sulfate-functionalized polyGGE. ATR-FT-IR spectra (**A**), TBO sulfate density analysis (**B**), and wettability (**C**) of unfunctionalized and sulfate functionalized polyGGE with and without autoclaving (_A), EtO gas (_E),

gamma-ray irradiation (_G) treatments (polyGGE, polyGGE_S15, polyGGE_S15_A, polyGGE_S15_E and polyGGE_S15_G). For **B**, n=8, for **C**, n=30, *p<0.05, one-way ANOVA with Bonferroni's multiple comparison tests.

Since the amount of grafted sulfate groups on polyGGE surface was in the nanomolar range (**Fig. 4B**), both DSC and TGA as the common techniques for studying the thermal properties of bulk materials are not sensitive enough for investigating the influence of the sterilization on sulfate-functionalized polyGGE.

In this context, poly(hydroxyethyl acrylate) (PHEA) hydrogel was synthesized [35] and functionalized with sulfates (PHEAS) to amplify the sulfation process and the influence of sterilization on sulfate groups as a model system. The reaction was illustrated in **Fig. 5A**. Physicochemical and thermal characterization of PHEAS after the autoclaving (PHEAS_A), EtO sterilization (PHEAS_E) and gamma-ray irradiation (PHEAS_G) was performed.

ATR-FT-IR was used to study the influence of sterilization on the chemical bonding of sulfates. Newly formed peaks after the modification were found at the location of 1216, 1019, 922, 840, 756 and 625 cm^{-1}. Similar to the results of polyGGE (**Fig. 4A**), EtO sterilization and gamma-ray irradiation had limited influence on PHEAS whereas all aforementioned peaks were significantly reduced after autoclaving (**Fig. 5B**).

The hydrophilic level of the chain segments of the hydrogel as well as its crosslinking density are reflected by its water uptake capacity. In **Fig. 5C**, the water uptake ability was significantly improved by sulfation of PHEA. EtO sterilization and gamma-ray irradiation showed no influence on the water uptake of PHEAS. In contrast to that, the water uptake of autoclaved PHEAS showed even lower water uptake than the original PHEA, which might due to additional crosslinking by transesterification and substantial loss of sulfate groups at elevated temperature.

TGA profiles showed that the degradation of PHEA initiated from 250 °C and completely decomposed at about 440 °C. Nonetheless, PHEAS presented a three-step decomposition process. Despite the minor weight loss before 100 °C, the first step of decomposition occurring between 130 °C and 150 °C was found. The second decomposition step started at 250 °C till 300 °C followed by the last decomposition started at 400 °C and completed at the same temperature as PHEA. PHEAS after EtO sterilization, gamma-ray irradiation showed the similar degradation behavior as unsterilized PHEAS. Interestingly, a unique decomposition curve was observed in autoclaved PHEAS when compared to both non-functionalized PHEA

and unsterilized PHEAS. Weight loss of autoclaved PHEAS continuously increased from 130 °C and the major decomposition was observed from 250 °C till 460 °C, leaving 9 wt% residues. Comparing to that, 27 wt% of indecomposable components was found for PHEAS, PHEAS_E as well as PHEAS_G (**Fig. 5D**).

Considering the degradability of PHEAS was above 100 °C, the heating temperature range of DSC analysis was set between -30 °C to 100 °C. At dry state, based on the curves of second heat run, T_g = 47 °C was determined for unsterilized PHEAS, which was two folds higher compared to non-functionalized PHEA (T_g = 14 °C). T_g values for PHEAS_E and PHEAS_G were 51 °C and 43 °C, respectively, while PHEAS_A had a T_g of 28 °C (**Fig. 5E**). These results suggest that sulfates in the network hinder the mobility of the chains, and autoclaved PHEAS showed relatively higher chain mobility than unsterilized PHEAS, EtO sterilized and gamma-ray irradiated PHEAS due to the loss of the sulfates.

Together, sulfate groups were not thermally stable independent of the substrate materials and the decomposition of sulfates occurred at around 100 °C. Autoclaving leads to the loss of sulfates. Although gamma-ray irradiation showed no severe impact on sulfates, a color change to brown indicates an intrinsic change might exist on sulfate-functionalized polyGGE films. EtO gas sterilization can be considered as one appropriate method for sterilization of the sulfate-functionalized polymers. There was no impact of EtO sterilization on sulfate group density, hydrophilicity, and thermal property and stability of the functionalized surface.

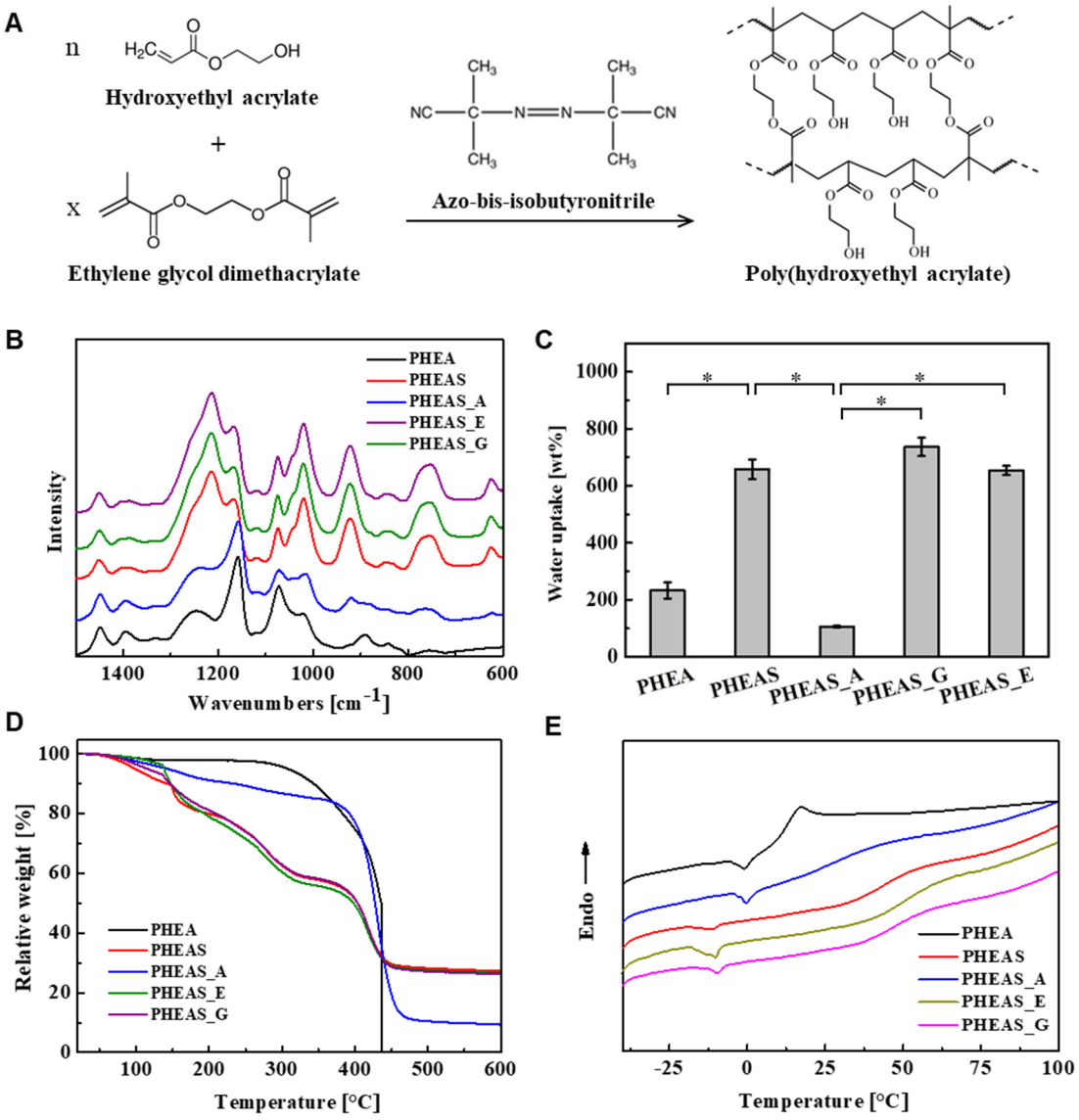

Fig. 5. Autoclaving reduced the sulfates in the poly(hydroxyethyl acrylate) (PHEA) hydrogel model system. A. Schematic illustration of the synthesis of PHEA. ATR-FT-IR spectra (**B**), water uptake (**C**), TGA (**D**) and DSC (**E**) curves of unfunctionalized and 15 min sulfate functionalized PHEA with and without autoclaving (_A), EtO (_E), gamma irradiation (_G) treatments (PHEA, PHEAS, PHEAS_A, PHEAS_E and PHEAS_G). For **C**, n=4, *p<0.05, one-way ANOVA with Bonferroni's multiple comparison tests.

Conclusions

Grafting of sulfate groups on the polymer surface was successfully carried out by reacting polyGGE with sulfamic acid in N-Methyl-2-pyrrolidone solution and can be stabilized by saturated NaCl treatment. Sulfation within 15 min guaranteed the sulfating process only took place on the surface while not occurring in the bulk of the polymer. The sulfate-functionalized polyGGE was thermal stable and flexible at the body temperature, while decomposition started after heating up over 100 °C. The diminished -C-O-S- and S=O peaks, reduced wettability as

well as impaired water uptake were observed on sulfate-functionalized polyGGE films post autoclaving due to the significant loss of sulfates. EtO can be considered as one of the appropriate techniques for sterilization of the sulfate-functionalized polymer networks. Sulfate functionalized poly(GGE) might develop a broad application spectrum in biomedicine derived from mimicking the natural sulfated cholesterol and glycosaminoglycans.

Acknowledgments

We thank Jorge Luis Escobar Ivirico, Manuela Keller, Susanne Schwanz, Thomas Weigel for technical support of PHEA synthesis, water contact angle, DSC, TGA and XPS analysis. This work was financially supported by the Helmholtz Association of German Research Centers (through program-oriented funding, Helmholtz Cross Program Initiative "Technology and Medicine Adaptive Systems", Helmholtz Virtual Institute, Multifunctional Biomaterials for Medicine (Grant no. VH-VI-423)) as well as by the Federal Ministry of Education and Research, Germany, through the Program Health Research (Grant no. 13GW0098).

References

[1] SoRelle R. Global epidemic of cardiovascular disease expected by the year 2050. Circulation. 1999;100(20):e101.
[2] Mendis S, Puska P and Norrving B, Global atlas on cardiovascular disease prevention and control, World Health Organization, Geneva, 2011.
[3] Piazza G and Goldhaber SZ. Venous thromboembolism and atherothrombosis: an integrated approach. Circulation. 2010;121(19):2146-50.
[4] Langford R, Hurrion E and Dawson PA. Genetics and pathophysiology of mammalian sulfate biology. J Genet Genom. 2017;44(1):7-20.
[5] Buono M and Cosma MP. Sulfatase activities towards the regulation of cell metabolism and signaling in mammals. Cell Mol Life Sci. 2010;67(5):769-80.
[6] Koning AM, Meijers WC, Minovic I, Post A, Feelisch M, Pasch A, Leuvenink HG, de Boer RA, Bakker SJ and van Goor H. The fate of sulfate in chronic heart failure. Am J Physiol-Heart C. 2017;312(3):H415-H421.
[7] Weitz JI. Heparan sulfate: antithrombotic or not? J Clin Invest. 2003;111(7):952-4.
[8] Seneff S, Davidson RM, Lauritzen A, Samsel A and Wainwright G. A novel hypothesis for atherosclerosis as a cholesterol sulfate deficiency syndrome. Theor Biol Med Modell. 2015;12:9.
[9] Mueller JW, Gilligan LC, Idkowiak J, Arlt W and Foster PA. The Regulation of Steroid Action by Sulfation and Desulfation. Endocr Rev. 2015;36(5):526-63.
[10] Strott CA and Higashi Y. Cholesterol sulfate in human physiology: what's it all about? J Lipid Res. 2003;44(7):1268-1278.
[11] Uyama T, Kitagawa H and Sugahara K, 3.05 - Biosynthesis of Glycosaminoglycans and Proteoglycans. in: Kamerling H, (Ed.). Comprehensive Glycoscience, Elsevier, Oxford, 2007;79-104.

[12] Akgul Y and Mahendroo M, 33 - Cervical Changes Accompanying Birth. in: Croy BA, Yamada AT, DeMayo FJ, and Adamson SL, (Eds.). The Guide to Investigation of Mouse Pregnancy, Academic Press, Boston, 2014;391-401.
[13] Mikami T and Kitagawa H. Sulfated glycosaminoglycans: their distinct roles in stem cell biology. Glycoconj J. 2017;34(6):725-735.
[14] Haroun-Bouhedja F, Ellouali M, Sinquin C and Boisson-Vidal C. Relationship between sulfate groups and biological activities of fucans. Thromb Rev. 2000;100(5):453-9.
[15] Clausen TM, Sandoval DR, Spliid CB, Pihl J, Perrett HR, Painter CD, Narayanan A, Majowicz SA, Kwong EM, McVicar RN, Thacker BE, Glass CA, Yang Z, Torres JL, Golden GJ, Bartels PL, Porell RN, Garretson AF, Laubach L, Feldman J, Yin X, Pu Y, Hauser BM, Caradonna TM, Kellman BP, Martino C, Gordts P, Chanda SK, Schmidt AG, Godula K, Leibel SL, Jose J, Corbett KD, Ward AB, Carlin AF and Esko JD. SARS-CoV-2 Infection Depends on Cellular Heparan Sulfate and ACE2. Cell. 2020;183(4):1043-1057.e15.
[16] Gray E, Hogwood J and Mulloy B. The anticoagulant and antithrombotic mechanisms of heparin. Handb Exp Pharmacol. 2012;207:43-61.
[17] Shriver Z, Raman R, Venkataraman G, Drummond K, Turnbull J, Toida T, Linhardt R, Biemann K and Sasisekharan R. Sequencing of 3-O sulfate containing heparin decasaccharides with a partial antithrombin III binding site. Proc Natl Acad Sci U S A. 2000;97(19):10359-64.
[18] Sasisekharan R and Venkataraman G. Heparin and heparan sulfate: biosynthesis, structure and function. Curr Opin Chem Biol. 2000;4(6):626-631.
[19] Eslamifar Z, Behzadifard M, Soleimani M and Behzadifard S. Coagulation abnormalities in SARS-CoV-2 infection: overexpression tissue factor. Thromb J. 2020;18(1):38.
[20] Burkel WE. The challenge of small diameter vascular grafts. Med Prog Technol. 1988;14(3-4):165-75.
[21] Park K, Mosher DF and Cooper SL. Acute surface‐induced thrombosis in the canine ex vivo model: Importance of protein composition of the initial monolayer and platelet activation. J Biomed Mater Res A. 1986;20(5):589-612.
[22] Wang Y-X, Robertson JL, Spillman WB and Claus RO. Effects of the chemical structure and the surface properties of polymeric biomaterials on their biocompatibility. Pharm Res. 2004;21(8):1362-1373.
[23] Lyman D, Metcalf L, Albo Jr D, Richards K and Lamb J. The effect of chemical structure and surface properties of synthetic polymers on the coagulation of blood. III. In vivo adsorption of proteins on polymer surfaces. ASAIO J. 1974;20(1):474-478.
[24] Absolom D, Zingg W and Neumann A. Protein adsorption to polymer particles: role of surface properties. J Biomed Mater Res A. 1987;21(2):161-171.
[25] Neffe AT, von Ruesten-Lange M, Braune S, Luetzow K, Roch T, Richau K, Jung F and Lendlein A. Poly(ethylene glycol) grafting to poly(ether imide) membranes: influence on protein adsorption and thrombocyte adhesion. Macromol Biosci. 2013;13(12):1720-9.
[26] Kastrup CJ, Boedicker JQ, Pomerantsev AP, Moayeri M, Bian Y, Pompano RR, Kline TR, Sylvestre P, Shen F, Leppla SH, Tang WJ and Ismagilov RF. Spatial localization of bacteria controls coagulation of human blood by 'quorum acting'. Nat Chem Biol. 2008;4(12):742-50.
[27] Ekinci D, Sisson AL and Lendlein A. Polyglycerol-based polymer network films for potential biomedical applications. J Mater Chem. 2012;22(39):21100.
[28] Paulus F, Steinhilber D, Welker P, Mangoldt D, Licha K, Depner H, Sigrist S and Haag R. Structure related transport properties and cellular uptake of hyperbranched polyglycerol sulfates with hydrophobic cores. Polym Chem. 2014;5(17):5020-5028.
[29] Al-Horani RA and Desai UR. Chemical Sulfation of Small Molecules - Advances and Challenges. Tetrahedron. 2010;66(16):2907-2918.
[30] Miller JJ. Cleavage of 1,3-Butanediol Cyclic Sulfate with Hydrogen Chloride. J Org Chem. 1962;27(7):2680-2681.
[31] Parreño RP, Liu Y-L, Beltran AB and Carandang MB. Effect of a direct sulfonation reaction on the functional properties of thermally-crosslinked electrospun polybenzoxazine (PBz) nanofibers. RSC Adv. 2020;10(24):14198-14207.

[32] Clapp LB. Sulfamic acid and its uses. J Chem Educ. 1943;20(4):189.
[33] Calderon M, Quadir MA, Sharma SK and Haag R. Dendritic polyglycerols for biomedical applications. Adv Mater. 2010;22(2):190-218.
[34] Li G, Yang P, Qin W, Maitz MF, Zhou S and Huang N. The effect of coimmobilizing heparin and fibronectin on titanium on hemocompatibility and endothelialization. Biomaterials. 2011;32(21):4691-703.
[35] Kyritsis A, Pissis P, Ribelles JLG and Pradas MM. Depolarization thermocurrent studies in poly(hydroxyethyl acrylate)/water hydrogels. J Polym Sci B Polym Phys. 1994;32(6):1001-1008.